PAPER • OPEN ACCESS

Plasma wakefield acceleration experiments at FACET II

View the article online for updates and enhancements.

IOP ebooks™

Bringing you innovative digital publishing with leading voices to create your essential collection of books in STEM research.

Start exploring the collection - download the first chapter of every title for free.

Plasma wakefield acceleration experiments at FACET II

C Joshi[1] , **E Adli**[2], **W An**[1] , **C E Clayton**[1], **S Corde**[3], **S Gessner**[4],
M J Hogan[5], **M Litos**[6], **W Lu**[7], **K A Marsh**[1], **W B Mori**[1], **N Vafaei-Najafabadi**[8],
B O'shea[5], **Xinlu Xu**[1,5], **G White**[5] and **V Yakimenko**[5]

[1] University of California Los Angeles, Los Angeles, CA 90095, United States of America
[2] University of Oslo, NO-0316, Oslo, Norway
[3] LOA, ENSTA ParisTech, CNRS, Ecole Polytechnique, Université Paris-Saclay, F-91762 Palaiseau, France
[4] CERN, Geneva, Switzerland
[5] SLAC National Accelerator Laboratory, Menlo Park, CA 90309, United States of America
[6] University of Colorado Boulder, Boulder, CO 80309, United States of America
[7] Department of Engineering Physics, Tsinghua University, Beijing 10084, People's Republic of China
[8] Stonybrook University, Stony Brook, NY 11794, United States of America

E-mail: joshi@ee.ucla.edu

Abstract

During the past two decades of research, the ultra-relativistic beam-driven plasma wakefield accelerator (PWFA) concept has achieved many significant milestones. These include the demonstration of ultra-high gradient acceleration of electrons over meter-scale plasma accelerator structures, efficient acceleration of a narrow energy spread electron bunch at high-gradients, positron acceleration using wakes in uniform plasmas and in hollow plasma channels, and demonstrating that highly nonlinear wakes in the 'blow-out regime' have the electric field structure necessary for preserving the emittance of the accelerating bunch. A new 10 GeV electron beam facility, Facilities for Accelerator Science and Experimental Test (FACET) II, is currently under construction at SLAC National Accelerator Laboratory for the next generation of PWFA research and development. The FACET II beams will enable the simultaneous demonstration of substantial energy gain of a small emittance electron bunch while demonstrating an efficient transfer of energy from the drive to the trailing bunch. In this paper we first describe the capabilities of the FACET II facility. We then describe a series of PWFA experiments supported by numerical and particle-in-cell simulations designed to demonstrate plasma wake generation where the drive beam is nearly depleted of its energy, high efficiency acceleration of the trailing bunch while doubling its energy and ultimately, quantifying the emittance growth in a single stage of a PWFA that has optimally designed matching sections. We then briefly discuss other FACET II plasma-based experiments including *in situ* positron generation and acceleration, and several schemes that are promising for generating sub-micron emittance bunches that will ultimately be needed for both an early application of a PWFA and for a plasma-based future linear collider.

Keywords: plasma accelerator, Facet II, low emittance beams, pump depletion, energy doubling

1. Introduction

For the past three decades various advanced accelerator schemes that push the properties of accelerators beyond the present limits of performance have been under investigation motivated by a desire to keep increasing the center of mass energy and luminosity of high-energy charge-particle colliders [1]. In order to make future colliders more compact and affordable, high-gradient, high-efficiency accelerators that generate ultra-bright beams are needed [2, 3]. Providing the required luminosity to support precision experiments in elementary particle physics will require a significant improvement in beam brightness. Such gains may therefore also enable next-generation coherent x-ray light sources. Of the many advanced ideas for high-gradient charged particle acceleration (inverse free electron lasers, dielectric structures and plasmas, for instance), the plasma accelerator scheme [4, 5] has unarguably made the greatest progress. This idea uses the extremely large electric fields (accelerating gradient) associated with a plasma wave moving at the speed of light to accelerate charged particles. The plasma wave or a wake is a disturbance left behind by an ultra short but ultra-intense charged particle bunch or a laser pulse [6]. The former is called a plasma wakefield accelerator (PWFA) while the latter is called a laser wakefield accelerator [7]. The laser pulse and the beam-driven plasma accelerators have many similarities but also have certain unique features. Both have succeeded in demonstrating acceleration of multi-GeV, narrow energy spread electron beams [8, 9]. The next decadal challenge [10] for the plasma accelerator community is to demonstrate a single stage of a multistage plasma-based tera electron-volt (TeV) scale accelerator. Preliminary design of a beam-driven plasma accelerator-based linear collider envisions that each plasma stage should increase the energy of the accelerating bunch by ~10 GeV and preserve its ultra-low emittance while nearly fully depleting the drive bunch energy [2]. In order to achieve this milestone a new facility, Facilities for Accelerator Science and Experimental Test (FACET) II [11] is being constructed at SLAC National Accelerator laboratory (SLAC).

In this paper we first discuss the present status of the beam-driven PWFA research carried out using the SLAC linear accelerator (linac) beams, followed by the description of the FACET II facility. This is followed by some key experiments that are proposed by the present authors on PWFA that are consistent with the decadal challenge for plasma-based accelerators mentioned above.

2. Present status of PWFA experiments using the SLAC linac electron (e^-) and positron (e^+) beams

In this section, we first describe the PWFA concept followed by a description of some of the key results obtained on two earlier facilities: the single bunch final focus test beam (FFTB) and the double-bunch FACET facility, hereafter referred to as FACET I.
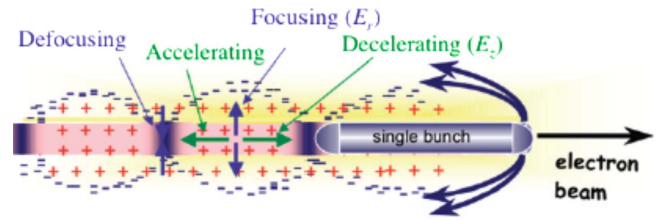

Figure 1. Concept of the PWFA using a *single* drive bunch. Note: for clarity, the transverse and longitudinal fields are indicated in second bucket but have the same signs and relative locations in all buckets.

2.1. PWFA concept and early results on the FFTB facility, 1998–2006

The basic concept of the PWFA involves the passage of an ultra-relativistic ($\gamma \gg 1$), short ($\sigma_z < \pi c/\omega_p$) and narrow ($\sigma_r < c/\omega_p$) bunch of charged particles through plasma [12]. Here γ, σ_z, σ_r and ω_p are the relativistic Lorentz factor, the rms bunch length and bunch radius and the plasma frequency respectively. The plasma can be formed by ionizing a gas with a laser [13] or through field-ionization by the (transverse) Coulomb field of the relativistic electron bunch itself [14]. If the bunch density is much greater than the plasma density ($n_b \gg n_p$) the transverse Coulomb field at the very head of the bunch can expel all the plasma electrons radially away from the bunch, leaving a column of ions in its wake. However, the force of the ions prevents the electrons from moving too far resulting in a thin sheath of electrons surrounding both the bunch itself and the ions. This is known as the blowout regime of the PWFA [15, 16].

In a simplified description the plasma electrons will eventually return to the axis as shown in figure 1, overshoot the axis, and continue to oscillate as a plasma wave or wake. The longitudinal range of positions where the electrons cross the axis is typically much smaller than the length of the ion cavity and thus the density of these crossing electrons (the 'spike') can be 10's of times larger than the initial plasma electron density (which is equal to the ion density). There are several basic phenomena to note due to this interaction of the drive bunch, the expelled electrons, and the ion column or 'bubble'. First, the electric field due to the spike of high-density electrons at the back of the bubble and the absence of electrons within the bubble can be extremely large. Second, for a wake generated in a preformed plasma, the distance between the head of the drive bunch and this density spike remains constant so that there is no slippage between the accelerating electrons and the large field. And third, since most of the drive bunch remains within an ion channel, both the drive and the accelerating electrons can be guided well over a meter. Fourth, as long as the drive bunch remains ultra-relativistic, the wake structure does not evolve/change as the drive bunch propagates through the plasma. Fifth, once the plasma electrons are completely blown out, the focusing force inside the cavity $F_r = (E_r - B_\theta)$ is constant with the longitudinal position $\xi = z - ct$, and varies linearly with the radial position r within the cavity—a highly desirable field configuration for preserving the emittance of the accelerating bunch. The Penofsky–Wenzel theorem implies that the

accelerating force $F_z = -eE_z$ is thus constant with r at a particular ξ and all the particles in a given longitudinal slice of the bunch gain energy at the same rate. Taken together these factors imply that electrons in given longitudinal slice at ξ will experience the same field, irrespective of their transverse position over the entire length L_p [17] of the wake and thus gain an energy of $\Delta W = E_z * L_p$.

The early PWFA experiments at SLAC's FFTB facility were carried out using a single electron bunch ($\sigma_z < 30 \mu$m, $\sigma_r < 10 \mu$m) as shown schematically in figure 1. The transverse electric field of the bunch was used to form the plasma by tunnel-ionization. Once the plasma was formed, electrons in the main body of the bunch produced the wake and therefore lost energy to the wake, however electrons in the back of the bunch sampled the accelerating field of the wake and thus gained energy from the wake. These experiments culminated in the demonstration of energy doubling of some of the tail electrons from initial 42 to 85 GeV in less than one meter of plasma wake albeit with a continuous energy spread [18].

The first demonstration of acceleration of positrons in a plasma wave was similarly accomplished at the FFTB facility. The longer ($\sigma_z < 1.2$ mm) positron bunch was sent through a preformed, low-density plasma column where a linear wakefield accelerated positrons at the back of the bunch with an accelerating gradient of 50 MeV m^{-1} [19].

Aside from these acceleration experiments, the FFTB experiments showed envelope oscillations of an unmatched electron beam and the concept of beam matching [20, 21], centroid oscillations of an off axis bunch, betatron radiation emitted by off axis electrons in the ion cavity of the wakefield [22], generation of $e^- e^+$ pairs from the betatron x-rays [23], electron [20] and positron [24] beam focusing by a thick plasma lens and ionization trapping electrons in a highly relativistic wake [25].

2.2. Key results on the FACET I facility, 2010–2015

Following the successful FFTB experiments, which used the entire three km of the SLAC linac, PWFA experiments took a hiatus due to the construction of SLAC's x-ray free electron laser: the Linac Coherent Light Source or LCLS [26]. The LCLS took over the last km of the linac, leaving the first two km of linac available for advanced accelerator research (see figure 3(a)). A new experimental facility, referred to as FACET, was constructed at the end of the second km of the linac (see figure 3(b)). There was little change in the expected beam parameters as both electrons and positrons were deliverable with the same charge (2×10^{10} particles/bunch) but with a reduced energy of ~21 GeV. The other beam parameters at the plasma entrance were similar when operating in a single-bunch mode. The major change was that the double bend beam compressor used at FFTB was replaced at FACET I by a specially designed 'w'-shaped chicane. This chicane (see figure 4) would be key for performing two-bunch experiments with either electrons or positrons.
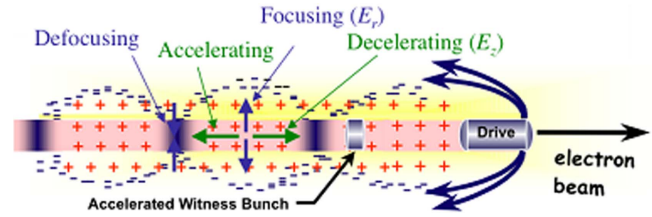

Figure 2. Concept of the PWFA using *separate* drive and witness bunches. Note: for clarity, the transverse and longitudinal fields are indicated in second bucket but have the same signs and relative locations in the all buckets.

The FACET I experimental area was specifically designed to generate a drive bunch followed by a witness bunch with variable spacing (on the order of the plasma wavelength for a density range of 10^{16} to a few 10^{17} cm^{-3}. In these two-bunch FACET I experiments, the two-km linac was set up such that a single electron/positron bunch entered the experimental area with a correlated energy spread; that is, a head-to-tail energy chirp. The first dipole magnet of the 'W-chicane' then disperses this chirped bunch horizontally (x-direction). At the point of maximum dispersion, an appropriate mask—a titanium wedge of variable width and thickness—is inserted into the central portion of the now energy correlated bunch (energy versus x). The mask scatters electrons in the central portion of the dispersed bunch allowing the unaffected high- and low-energy portions to continue through the chicane where they are slightly over-compressed but back on the same axis (note: in addition to this Ti-wedge two additional titanium blades, insertable at the high- and low-energy positions of the dispersed bunch were often used as well to manipulate the charge at these energy extremes). Thus a single bunch becomes two bunches with the lower energy (drive) bunch exiting the chicane first. By changing the incoming chirp on the bunch, the bunch spacing can be also changed. The drive bunch, typically containing 1.5 nC of charge, is followed by the witness (also called the trailing) bunch containing ~250 pC of charge. The drive and the trailing bunches are typically ~50–100 fs (FWHM) in duration and separated by about 0.5 ps. By remotely manipulating the titanium masks mentioned above, the charge of either bunch and/or the charge ratio between them can be controlled. Moreover, either bunch can be 'blocked' at will.

The FACET I experiments carried out using such a double-bunch configuration (shown schematically in figure 2) have demonstrated that a significant fraction of the energy that the drive bunch loses to the wake can be gained back by the trailing bunch. This implies that the presence of the trailing bunch reduces, or 'loads', the accelerating electric field of the wake. With this loading, the total energy contained in the wake is reduced and given to the trailing bunch; a measurement of this is a measure of the efficiency of the acceleration process. Also, if the trailing bunch containing a certain charge is placed at some optimum position behind the drive bunch, the loaded electric field can be 'flattened' at that location such that most of the trailing bunch experiences the same accelerating field. Thus, an initially narrow-energy
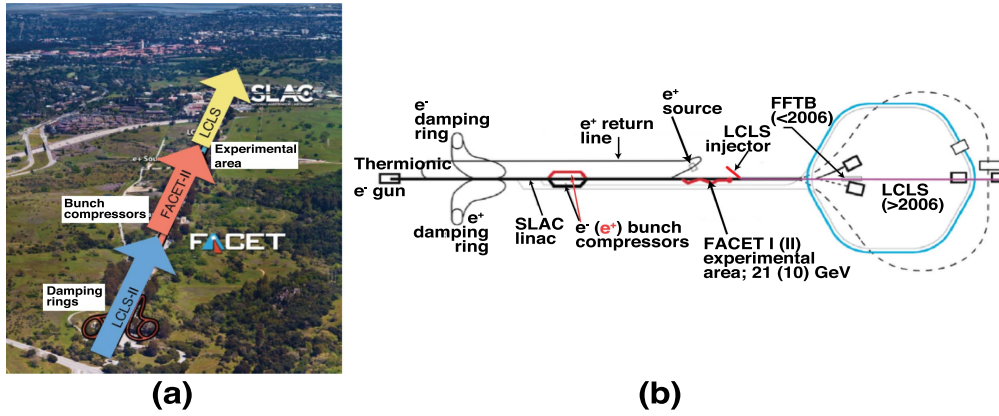
(a)

(b)

Figure 3. (a) The three km of the original linac will be dedicated to three facilities as indicated: LCLS (operational with 'first light in early 2009) powered by the final km of the SLAC linac; LCLS II currently under construction, to be powered using new accelerator components in the first km of the SLAC tunnel, displacing a km of linac used in FACET I; and, FACET II (under construction) powered by the center km of the linac. (b) A schematic of the SLAC site (circa 2005; pre-LCLS). Also shown with red lines are the positron bunch compressor, the FACET I experimental facility commissioned early 2011, and the location of the LCLS injector.

trailing bunch will experience a small increase of its energy spread (as will be discussed further in section 4.3). For this experiment, it was found that the efficiency of transferring drive bunch energy to the core of the accelerated bunch was up to 30% [8]. Clearly optimum beam loading (flattening of E_z) and increase in energy spread are intimately related. To date a maximum energy gain of 9 GeV for a bunch containing 80 pC of charge with a 5% energy spread in a 1.2 m long plasma has been observed [27].

We also showed that the PWFA cavity in the nonlinear blowout regime has the longitudinal and transverse field structure that in principal will accelerate electrons without emittance growth [17]. However the electrons (to be accelerated) have to be matched in and out of the plasma as we shall later see. The plasma wake produced by an electron bunch cannot be used to accelerate a positron beam when the wake is in the nonlinear blow out regime because the plasma ions strongly defocus the positrons. In fact it was not very clear how efficient positron acceleration at a high gradient could be carried out using highly nonlinear plasma wakes. We found that for a given plasma density, a certain positron beam current profile and bunch length can lead to a loaded wake where the electric field reverses sign (from decelerating to accelerating) in the middle of the single drive bunch [28]. This happens because the presence of the positrons pulls in the plasma electrons towards the axis. These plasma electrons cross the axis in the middle of the drive bunch. Most of the electrons overshoot and set up a bubble like wake cavity but a significant fraction of the electrons are confined by the back of the positron beam close to the axis. This flattens the wake shape by beam loading [28]. A significant amount of positron charge is now accelerated at the same electric field gradient producing a well-defined narrow energy peak in the accelerated spectrum. The energy extraction efficiency is similar to the electron bunch acceleration case described above.

In addition we have demonstrated generation of wakes and acceleration of a distinct positron bunch in a preformed plasma [29] and in a hollow channel plasma [30, 31]. We have also quantified the magnitude of the transverse

wakefields that are excited by a misaligned beam inside a hollow plasma channel [32].

3. The FACET II facility

In 2016, FACET I ceased operation to make way for the LCLS II facility that will occupy the first one km space of the original SLAC linac tunnel. A new facility for advanced accelerator research, known as FACET II, is being constructed between the LCLS II linac and the LCLS I linac as indicated in figure 3 [11]. The FACET II experimental area will be in the same location as that of FACET I. The FACET II facility is designed to be a versatile facility for advanced accelerator research and development. By offering pulse charge from pC to several nC, emittance from sub to ten microns, electrons and positrons, single and double bunches, tailored profiles with peak current up to nearly 100 kA and energy up to 10 GeV, FACET II provides ultrarelativistic beam capabilities unparalleled anywhere in the world. The FACET laser system is capable of providing multi-terawatt peak powers with state of the art synchronization between the electron bunch and the laser pulse approaching 30 fs.

Because FACET II will utilize only the middle, one km of the original SLAC linac, the beam energy will be reduced from 21 GeV in FACET I to 10 GeV in FACET II. This is not a concern, however. The lower drive bunch energy of 10 GeV in FACET II will enable a more definitive demonstration of the total drive beam to trailing beam energy transfer efficiency by energy depleting a significant fraction of the energy contained in the drive bunch in a meter-scale plasma. Most importantly, the expected beam quality for FACET II is far superior to its predecessor due mainly to a new electron bunch source. A radio-frequency (RF) gun will replace the thermionic gun plus damping rings shown in figure 3(b) allowing for the delivery of a very low emittance beam to the interaction point (the plasma). This in turn means that the final focusing quads will be able to focus the FACET II beam to a much smaller spot size (3–4 μm) thereby allowing the
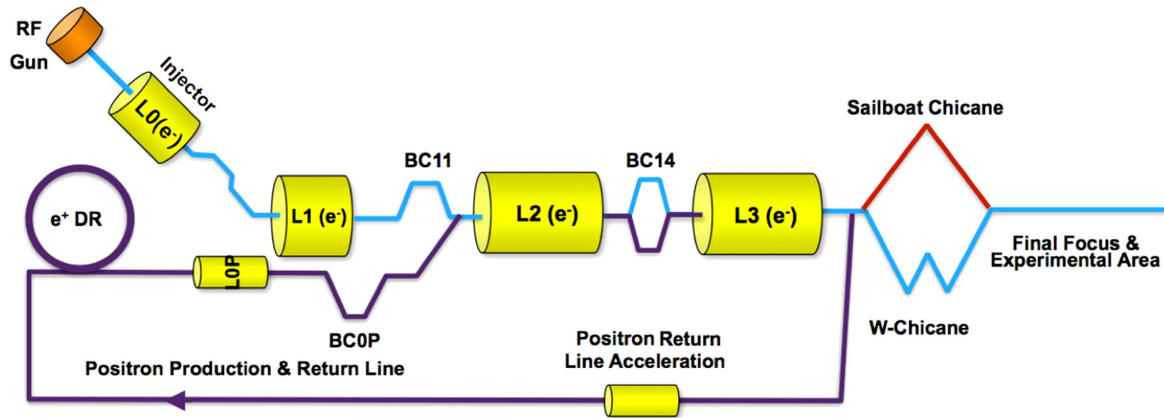
4

Figure 4. A schematic showing the design of the FACET II (using a spur in the tunnel to house a new photoinjector, pre-accelerator L0, and optional chicane for laser heating) along with rearranged SLAC linac sections (Ln(e^-), $n = 1, 2, 3$) and bunch compressors BC11 and BC14 capable of providing 10 GeV electrons to the 'W-chicane' (to be replaced by a double-dogleg chicane as in figure 5(b)) and experimental area. Also shown in purple are the positron production and return lines, the positron damping ring, a $-90°$ off-crest RF section for chirping the positrons (L0P), and the positron bunch compressor (BC0P). When injected into linac L2, the positrons will have a similar energy, bunch length, and charge as for the electrons. The red lines indicate the 'sailboat' chicane to bring positrons to the interaction point on the same event as the electrons.

Table 1. Comparison of bunch parameters for the two input bunches (drive and trailing) and the output bunch (accelerated trailing bunch) at the interaction point and exit of the plasma, respectively, for the earlier FACET I facility and for the expected (nominally) FACET II operation.

	Facet I (delivered) [27]	FACET II (expected/simulated)
Drive bunch		
Drive and trailing energy	21 GeV	10 GeV
Charge/σ_z/I_{peak}/σ_r	600 pC/30 μm/ 6 kA/30 μm	1.6 nC/13 μm/ 15 kA/4 μm
$\delta E/E$	0.8% r.m.s	0.15% rms
Normalized emittance	200 $\times$ 50 μm (with Be foil)	<7 $\times$ 3 μm (without Be foil)
Trailing bunch		
Trailing Energy	21 GeV	10 GeV
Charge/σ_z/I_{peak}/σ_r	350 pC/50 μm/ 2.1 kA/30 μm	0.5 nC/6.4 μm/ 7.5 kA/4 μm,
$\delta E/E$	1.5% rms	<1% rms
Accelerated bunch		
Final energy spread	<5%	1%
Energy gain	9 GeV (max)	>10 GeV
Efficiency	30% (max)	50%
Emittance preservation	No	Yes

beam to be matched to the plasma. A schematic of the new facility is shown in figure 4 and a comparison of the FACET I and the expected FACET II beam parameters is summarized in table 1.

As indicated in figure 3(b), the LCLS RF photoinjector gun (LCLS injector) is located in a spur off the main tunnel. The FACET II RF gun will similarly be located in another spur as indicated in figure 4. All the LCLS experience will be available for this RF gun as well as for the accelerator modules (Ln(e^-) in figure 4) and soft-bend chicanes beyond. The beam from the gun will be accelerated to ~ 0.14 GeV before the bunch turns into the main tunnel. With this low starting energy, tight control of the bunch's longitudinal phase space is obtained by appropriately phasing the remaining klystrons in conjunction with the two chicanes (bunch compressors) in the main tunnel. This will provide highly adjustable final (prior to the final-compression chicane) longitudinal bunch parameters, even at high currents.

Also shown in figure 4 is a schematic of the proposed, future positron beamline. The positron source will be the same as that in figure 3(b), but now sent to a new, compact damping ring. The so-called 'sailboat chicane', in addition to functioning as a compressor for positrons, it can be used to send e^+ and e^- bunches into the plasma 'simultaneously' with a variable delay; that is, with the positrons arriving plus/minus a plasma period with respect to the electrons.

The improved beam parameters (as seen by start-to-end 6D particle tracking simulations using ELEGENT, that include coherent synchrotron radiation and wakefield effects) at the final focus are not due solely to the vast improvement offered by the RF gun and robust phase-space manipulation, but also to a redesign of the final compressor. As shown in figure 5(b), the new final-compression chicane will be a 'double-dogleg', eliminating two dipoles and several quadrupoles compared to the W-chicane. Although less versatile in some respects, for example, R56 tuning, the reduced dipole strengths and larger beam pipes will allow the delivery of bunches with up to 175 kA with only a small increase of the emittance (e.g., from $\varepsilon_y \sim 3$ to ~ 7 μm). Moreover, a low-beta orbit has been designed that will improve the chromaticity of this chicane. An example of a high-current, two-bunch phase space is shown in figure 6 suggesting that we can go well beyond the parameters of table 1, opening up a much
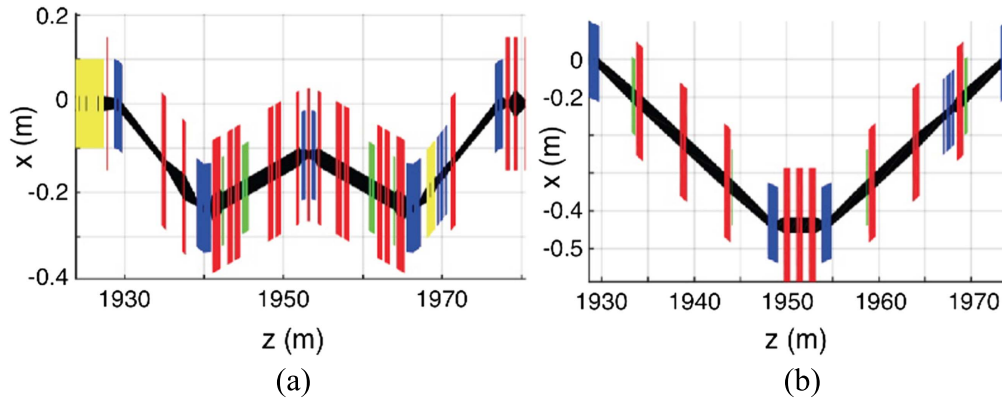
Figure 5. Existing final electron compression chicane (a) and its redesigned version with fewer magnets (b). Quadrupole magnets are shown in red, bends are in blue, sextupoles are in green. The yellow boxes in (a) show the accelerating structures at the end of the linac and the transverse cavity (the so-called T-CAV, essentially an *x*-band 'streak camera') in the chicane. For the re-designed optics, the transverse cavity is included in the beamline downstream of the chicane.

wider range of possible experiments. The energy-selective tantalum inserts used in Facet I to produce two bunches and bunch diagnostics will be retained in FACET II.

There are two alternatives for a trailing bunch source that would not require 'splitting' the single, chirped electron bunch from the RF injector thereby losing charge. The first option considered is a standalone, 100–300 MeV high-brightness source that could possibly deliver ultra-short trailing bunches of a variety of longitudinal current profiles immediately after the drive bunch. The main advantage would be to separate common-mode effects of using the same source for both driving and diagnosing the PWFA with bunches that have the same overall beam transport line. Also, given the energy disparity, the drive and trailing bunches can have different Twiss parameters at the plasma entrance and, of course, different offsets in position and in angle. However, for experimentally modeling a single stage of an energy-frontier-relevant collider pushes the limits in making of such a trailing bunch. For example, for $>10\,\mathrm{GV\,m^{-1}}$ fields, the plasma densities of interest are too high for the available $\sim 2.4\,\mathrm{kA}$ peak current from such a source to effectively load the accelerating wake. The second of these independent trailing-bunch schemes would be to utilize the LCLS II beam that will be present in an overhead beam pipe as it passes through the middle km of the SLAC tunnel. This 4–8 GeV beam could be diverted at up to 30 Hz down into the FACET II portion of the tunnel and 'doglegged' onto the main line of the linac. A separate trailing bunch could elucidate any effects of possible (upstream) drive-beam variations that propagate down to the plasma entrance via a now upstream-independent trailing bunch. Both of these options are not needed for the science experiments on PWFA discussed below.

4. PWFA program at FACET II

It is recognized by the scientific community that a future linear collider operating at the frontier of particle physics is both a scientific and engineering grand challenge for this

century [33]. In 2016, the US Department of Energy's Office of High Energy Physics (DOE-HEP) arranged a workshop to develop a long-range strategic development plan for advanced acceleration concepts R&D [10]. This report laid out milestones that would enable optimal use of the various facilities best suited to address a particular set of problems. The ultimate goal of the long range planning exercise is to address as many of the physics problems as existing facilities will allow and identify all the engineering issues to enable a technical design report for a collider operating at the energy frontier of particle physics based on one of these advanced accelerator concepts by 2035. It was recognized that demonstrating a 'near-term' application of the leading concept was important for proving the validity, technical readiness and usefulness of the scheme and for generating the considerable resources that will be needed to build a prototype accelerator for the linear collider application.

In response to this report the PWFA collaboration has come up with an initial, five-year R&D plan for FACET II that is consistent with the DOE-HEP's strategic plan mentioned above. As mentioned earlier, the decadal goal of this plan is to demonstrate (as much as the FACET II facility allows) electron beam parameters expected from a single stage of a future multi-stage PWFA-based linear collider (PWFA-LC). It should be noted that the design of a PWFA-LC itself is a multi-parameter problem and that optimization of the design must take into account limitations on some of these parameters that only experiments can reveal. We have broken up the decadal goal of this program into several smaller goals with the intention that all these goals can be simultaneously achieved in a single integrated demonstration within the decade. We first list the five-year goals and then discuss them one by one.

The first goal is to show that the 10 GeV drive bunch can be substantially depleted of its energy with drive beam to wake energy transfer efficiency >80%. The second goal is to demonstrate that the trailing bunch can gain at least 10 GeV energy in less than 1 meter from a single stage of PWFA. The third goal is to show that this 10 GeV energy gain can be
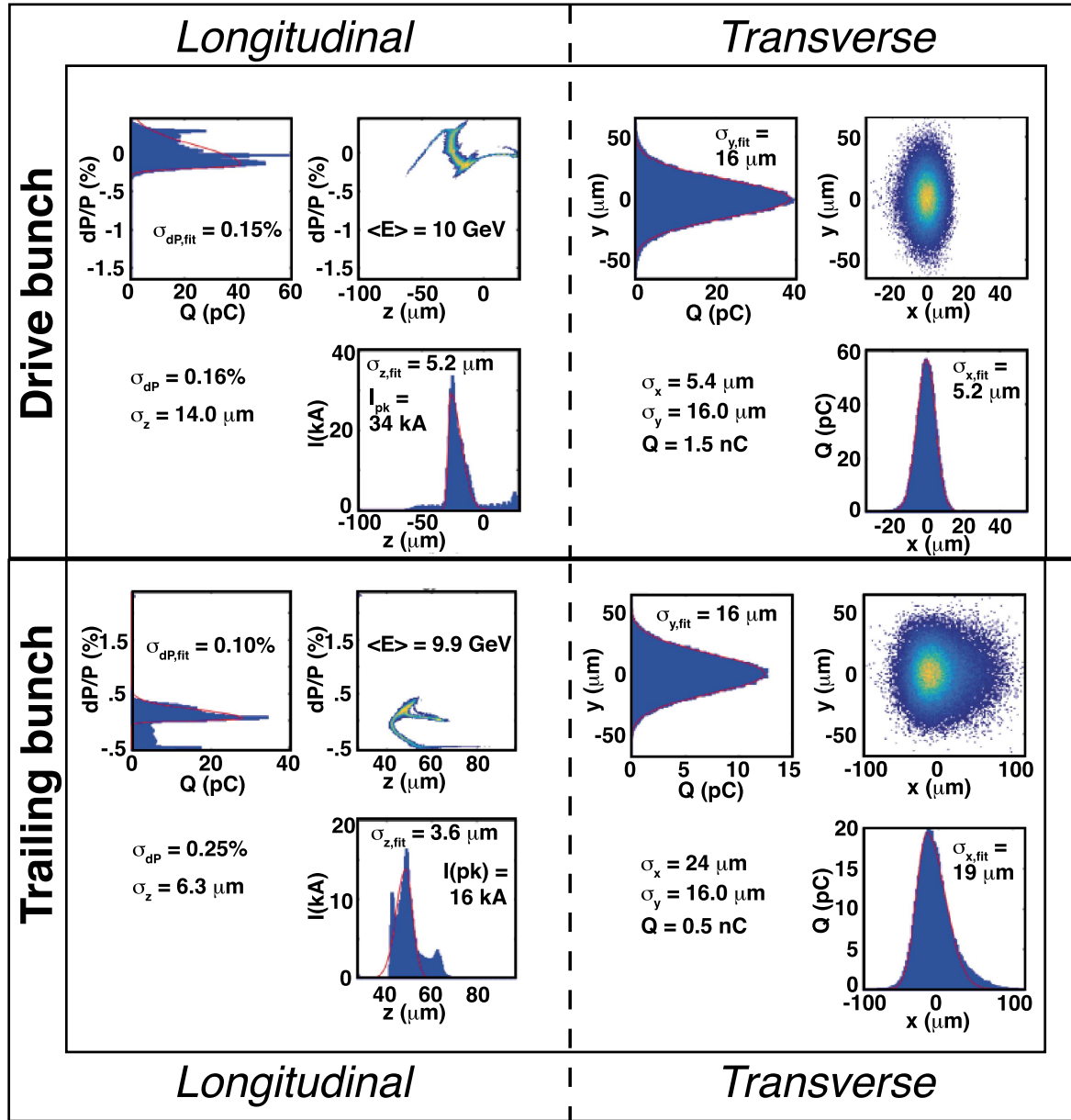
Figure 6. Results of 6D particle tracking, shown at the interaction point (IP), after tracking the particles from the RF gun to the IP (entrance to the plasma). Drive (witness) beams have *x* by *y* emittances of 7.2 × 3.2 μm (7.4 × 3.0 μm) which, for this simulation, have about twice the peak current in both bunches with respect to the minimum performance initially requested by PWFA experimentalist via 3D PIC simulations (see table 1).

obtained while extracting 50% of the energy stored in the wake, i.e., a net drive bunch to the trailing bunch energy transfer efficiency of 40%. A forth goal is to show that the trailing bunch energy spread is kept to below 2%. A fifth goal is to demonstrate the emittance preservation of a low emittance trailing beam as it gains 10 GeV in a single stage. If the emittance growth occurs, then identify the various factors (e.g. beam mismatch, incomplete blow out, asymmetric beams, transverse instabilities, ion motion etc) and propose mitigation strategies. Finally, carry out experiments that will generate beams with a brightness that will be required for colliders and for possible early application of a PWFA bunch. Of these goals, emittance preservation is one that is likely to prove the most challenging and therefore is discussed in some detail in section 4.3.

In the following sections, we show how these goals can be accomplished by modeling much of the proposed program using the 3D code QuickPIC. Initial simulation results will be displayed using the drive bunch and the trailing bunch parameters shown in table 1. The simulation uses an 80 cm long plasma with a density of 4×10^{16} cm^{-3} with appropriate density ramps to match the beams in and out of the plasma with the bunch separation being ∼150 μm. The two-bunch structure in this case would be produced by using the W-chicane and tantalum inserts described earlier. Alternatively, we have the option of double-pulsing the RF photocathode with a pair of laser pulses and use the RF-phase-dependent energy differential of the two pulses and the energy-dependent time-of-flight in the chicanes in main beam line to adjust the bunch separation down to about 75 μm

while compressing each pulse an additional factor of two. The particle-tracking simulation of figure 6 shows this case. Here, the required plasma density would have to be increased by a factor of four over the baseline design of 4×10^{16} cm^{-3}. The accelerating gradient would be a factor of two larger and the pump-depletion would occur in half the distance compared to the case considered below.

4.1. Pump depletion

A PWFA-LC for HEP applications will need to have a high overall or wall-plug efficiency η. This in turn is a product of several factors; $\eta = \eta_{\text{ac-db}} \, \eta_{\text{db-wake}} \, \eta_{\text{wake-tb}}$. Here $\eta_{\text{ac-db}}$ is the wall plug electrical energy that is converted into the drive bunch kinetic energy, $\eta_{\text{db-wake}}$ is the energy transfer efficiency from the drive bunch into the wake, and $\eta_{\text{wake-tb}}$ is the efficiency of energy extraction from the wake into the trailing bunch. Maximizing any of these three efficiencies will give some leeway for designing the collider. The optimization of $\eta_{\text{ac-db}}$ is beyond the scope of this paper and will therefore not be discussed here. If we assume that energy recovery of the unspent drive beam is undesirable because of the added complexity and expense, then we should maximize $\eta_{\text{db-wake}}$. This in turn means that for a single stage of the accelerator, as much of the drive beam energy should be transferred to the wake as possible. It has been shown that by shaping the drive beam current profile [34] it is possible for nearly all the particles in the drive beam to lose energy at the same rate (E_z^+ constant). However in the early years of operation, precisely shaped beams will not be available at FACET II. But even a Gaussian current profile ultra-relativistic bunch can transfer most of its energy to the wake [34] before the energy depletion (pump depletion) effects begin to slow the phase velocity of the wake—an undesirable effect.

For similar plasma-density and drive bunch parameters that we propose to use, we have seen the drive bunch drop from 21 GeV to about 4 GeV over ~1.4 m in FACET I experiments. Therefore a 10 GeV bunch should lose nearly all the energy to the wake in less than 1 m. However, in those experiments, the plasma was preformed by laser ionization. In these experiments, we will use higher peak-current bunches than in the previous experiments allowing us to generate the plasma using tunnel ionization by the transverse electric field of the beam itself. This raises the issue of beam head erosion possibly limiting the energy transfer to the wake. These issues can only be checked through simulations. For instance we found that after propagating through a total length of 85 cm (50 cm of flat density region plus the density ramps) of self-ionized plasma the drive beam lost >80% of its energy to the wake without any significant phase slippage between the accelerating bunch and the wake.

4.2. High efficiency, 10 GeV gain

After optimizing the drive bunch energy transfer to the plasma wake we wish to show that the trailing bunch can extract half of the energy from the wake at a loaded accelerating gradient of >10 GeV m^{-1}. In addition we wish to show that the energy spread of the bunch can be kept below 2% (rms).

In section 4.1, we described how we might find the best coupling of the drive beam to the wake in order to fully deplete its energy. For each optimal plasma density and drive bunch current profile, there is an optimum separation between the drive and trailing bunches to significantly reduce (load) the E_z field of the wake at the location of the trailing beam so that the energy stored in the wake is efficiently transferred to the witness beam. Again, as in the case for the drive bunch, there is an optimum bunch shape (trapezoidal, where the bunches charge density is large at the front and falls away at the back) for exact flattening of the wake. The reason for this is that, even though the wake's electric field E_z^- increases with ξ, the bubble radius r_b decreases (as one moves from the center towards the back). Thus the local volume of the field seen by a particular slice—and thus the energy available to transfer to that slice—decreases as r_b^2. For the energy spread of the trailing bunch to be kept small, the trailing bunch should have a higher current at the front (large r_b) compared to the back (small r_b) to flatten the E_z^- field. This is what gives the trapezoidal current profile.

In our simulations we use a Gaussian trailing bunch to beam load the wake. After optimization we found that the E_z^- field is flattened in the vicinity of the peak current region, figure 7(a), that contains most of the particles, extracting ~50% of the energy from the wake at a gradient of 15 GeV m^{-1}. The QuickPIC simulation result shown in figure 7(b) shows how at 65 cm of propagation, while the drive beam is pump depleted, the trailing bunch energy has increased from 10 GeV to approximately 21 GeV. Furthermore (although not seen here) the wake does not evolve significantly throughout propagation through the plasma. The rms energy spread of the trailing bunch at this point is less than 2% and the trailing bunch extracts ~50% of the energy from the wake; i.e., $\eta_{\text{wake-tb}}$ is 50%.

In the following section, we discuss our plans to minimize emittance growth by using a matching section of plasma before and after the acceleration portion of the plasma while keeping the energy spread small.

4.3. Energy spread and emittance preservation

Any residual energy spread will lead to some projected emittance growth of the beam. However, this is minimized if the beam is 'matched' into the plasma. A beam-slice of a given energy is matched if its tendency to diverge due to its emittance (the 'emittance force' in the beam envelope equation) is balanced by the attractive force due to ion focusing. Thus, the transverse size of a bunch slice, when matched, will be given by $\sigma_{\text{rm}} = (\varepsilon_n \, (c/\omega_p) \, (2/\gamma)^{1/2}))^{1/2}$ and this slice will not oscillate in size. Here, ε_n is the normalized emittance, ω_p is the plasma frequency, and γ is the Lorentz factor associated with the beam's energy.

We have experimentally shown that the PWFA in the fully blown out region has the field structure to preserve the emittance of the beam. That is, the variation of the focusing
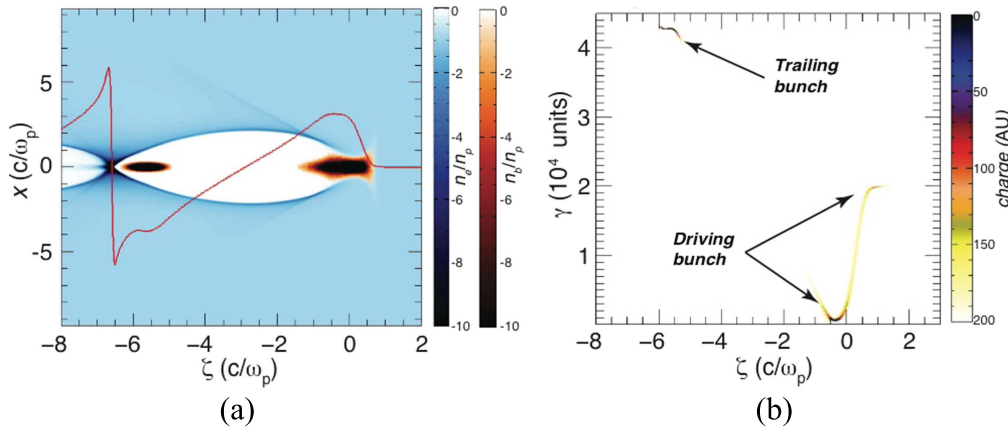
Figure 7. (a) The plasma and beam density along with the on-axis electric field showing the flattening of the E_z field due to beam loading. The drive and the trailing bunches are propagating from the left to right. Here the drive bunch produces the plasma and excites the wake. The very front of the drive bunch is seen to expand because of the beam's emittance. (b) Particle plot showing the energy depletion of the drive beam and the energy doubling of the trailing bunch while maintaining a small energy spread. Plasma density $4 \times 10^{16}\,\mathrm{cm}^{-3}$ with a 50 cm flat density region and 10 cm scale-length density ramps to match the beams in and out of the plasma. For this PIC simulation (and for the numerical calculations discussed in section 4.3 below), the drive and the trailing bunches, each having 10 GeV energy, $\varepsilon_{\mathrm{N}} = 10\,\mu$m, and an initial spot size of $\sigma_r = 21.2\,\mu$m, $\beta = 89.61$ cm, $\alpha = 0.0653$, were focused to $\beta^* = 3.9$ cm and $\sigma_r^* = 4.4\,\mu$m. The bunches gradually further focused to a matched beam size of 1.6 μm. The peak current (charge) of the drive bunch is 15 kA (1.6 nC) and the trailing bunch is 9 kA (0.5 nC). The two bunches are separated by 150 μm.

force with longitudinal position within the trailing bunch is zero; i.e., that each electron within a slice of the trailing bunch oscillates about the axis at the same betatron frequency. Moreover, each electron in that slice will see the same accelerating field. This is true whether the trailing bunch is matched or not. However, if an unmatched trailing bunch has a substantial energy spread due to imperfect flattening (loading) of the E_z^- field, a neighboring slice will have a different betatron frequency as this frequency varies as $\gamma^{-1/2}$. These neighboring slices, having different betatron frequencies and thus a different phase advance at a given instant, will each project onto an ellipse in transverse phase space that will be rotated with respect to the one another. The area of the smallest encompassing ellipse, a measure of emittance, will thus be larger and will grow as the bunch propagates indicating a growth in the projected emittance.

Since an ion channel of a PWFA operating at densities of interest to FACETII will have an extremely large focusing force (O(MT/m)) a conventional magnetic optic will be too weak to focus the beam to its matched spot size σ_{rm}. In practice the beam will have a small energy spread and therefore the matched spot size is defined at the centroid energy of the beam. In an experiment, the longitudinal profile of the plasma is not rectangular. There are up- and down-ramps at the entrance and exit of the uniform density section of the plasma. The emittance of the incoming beam has to be preserved throughout the plasma, including the up- and down-ramps. Thus the accelerating or trailing bunch must be matched throughout the plasma. Once the trailing beam is within the flat-topped portion of the plasma profile, it must beam load the accelerating cavity such that its energy spread increases but a little so that the projected emittance of the beam is not rapidly increased. Thus the problem is reduced to beam matching for slice emittance preservation and beam loading for high efficiency, small energy spread and projected

emittance preservation. Fortunately, a properly engineered plasma up-ramp can gradually increase the large plasma focusing force in such a way that a conventional, external magnetic focusing optic can match the electron beam at the entrance of the plasma up-ramp (that is, a larger spot here will match to this low density) and the increasing focusing force of the wake in an increasing density keeps this beam matched by continuously squeezing it to a smaller spot size. The situation is reversed at the plasma exit.

The concept of a plasma matching section has been considered in several recent publications and was revisited in the context of a PWFA operating in the blowout regime by Xu *et al* [35]. In this work conventional magnetic optics produce a waist ($\alpha_i = 0$) with an initial beta β_i. This is shown in figure 8(a). Here, α_i and β_i are the Twiss/Courant Snyder parameters of the incoming beam brought to a focus in vacuum at the start of the matching section. By constraining the plasma profile such that the beam's beta is continuously matched in the profile and that, once in the flat-topped region (labeled PA for plasma accelerator), $\beta_{\mathrm{goal}} = \beta_{\mathrm{matched}}$ and $\alpha_{\mathrm{goal}} = 0$, the bunch is matched to the uniform, high-density region of the plasma. This approach requires engineering of the plasma source to have prescribed up-ramp and down ramp profiles.

To use an existing profile as plasma matching sections puts the onus on us to appropriately design the focusing (collection) optics to produce the requisite incoming (outgoing) beam Twiss parameters. The design of such a beam matching is carried out as follows. We desire that the bunch (es) have to be matched throughout the PA section. Since we know the plasma density and the beam energy at the input (and output) and emittance, we calculate the matched beam size at the input (output) of the PA and then numerically propagate the Twiss parameters backwards (forwards) towards the focusing (collection) optics by splitting each
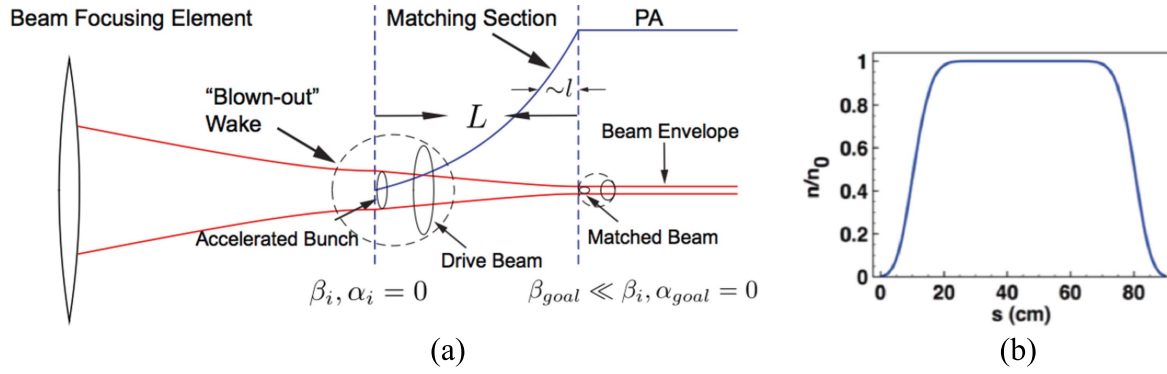
Figure 8. (a) A schematic of beam matching using a plasma density up-ramp at the entrance of a plasma accelerator [35]. The drive and the trailing beam are both focused at the entrance of the plasma density ramp. The drive beam produces a fully blown out wake. The focusing force of the ions at this point is matched by the emittance force of the electron bunch and thus the beam is matched to the plasma. As the focusing force is gradually increased the beam spot size is slowly compressed such that the beam is matched at the top of the plasma density ramp and is again at a waist ($\alpha_{goal} = 0$). Here, L is the total length of the matching section while l is the density scale length. (b) The plasma up- and down-ramps for a mid 10^{16} cm^3 atomic Li in a heat pipe oven. The profiles were obtained by converting position s-dependent temperature measurements into Li vapor pressure.
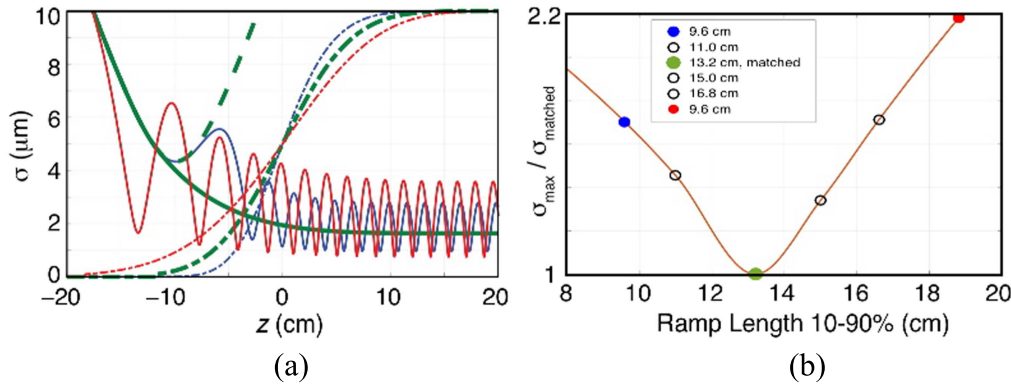

Figure 9. (a) An example of the determination of incoming beam parameters to match a particular profile (heavy green lines, see text) and the betatron oscillations of that same incoming beam if the profile were to change (red and dark-blue lines). (b) A summary of the maximum betatron spot size within the plasma normalize to the matched size for six profiles, three of which are shown in (a).

ramp into thousands of thin plasma 'lenses' with assigned strengths according to an analytic fit to the known ramp profiles such as those shown in figure 8(b). Eventually the plasma density in the ramps is so small that the bunches begin to expand as if propagating in vacuum with a spot-size evolution $\sigma_{r,\mathrm{vac}}(s)$ characterized by the parabola given by $(\sigma_{r,\mathrm{vac}})^2 = (\sigma^*_{r,\mathrm{vac}})^2 \quad (1 + ((s\text{-}s^*_{\mathrm{vac}})/\beta^*_{\mathrm{vac}})^2)$. Here, $\beta^*_{\mathrm{vac}} = (\varepsilon_n \, \sigma^*_{r,\mathrm{vac}})^{1/2}$, and the minimum vacuum spot size occurs at $s\text{-}s^*_{\mathrm{vac}}$ where $\alpha_{\mathrm{vac}} = 0$. The requirements on the conventional magnetic focusing (collection) optics are therefore more relaxed since the ramps do much of the work of continuously decreasing(increasing) the beam spot size. Thus, away from the bottoms of the ramps, one can then find the unique Twiss parameters that, if propagated from the conventional optics back towards the ramps, would follow a matched trajectory into the PA region. This procedure was used to find the incoming Twiss parameters for matching into the plasma for the PIC simulation of figure 7.

This is illustrated in figure 9(a) where a 10 GeV energy drive bunch was focused to a $\beta^* = 3.9$ cm ($\sigma_r^* = 4.4\,\mu$m) onto three different up-ramps, each having a different scale length. Only the 13 cm plasma scale-length profile, shown

with a heavy green dot-dashed curve, represents actual the experimental ramp profile for matched beam propagation. Once the incoming beam Twiss parameters were found by the backward-propagation method described above, the beam propagation direction was reversed again, now propagating in its normal direction. By numerically turning off the plasma, represented by the in the heavy green dashed parabola, we easily find the requisite vacuum waist location (σ^*) and beta function (β^* corresponding to a spot size of σ^*) that the incoming beam (from the final focus optics) must have to match throughout the up-ramp. Finally, after numerically restoring the plasma forces, we see that this beam has indeed the proper Twiss parameters—its beam envelope size smoothly shrinks from its vacuum focus size until it is matched to the plasma (heavy green solid curve) with no envelope (or betatron) oscillations within either the ramp or the PA region. Also shown, for that same incoming beam, how the envelope behaves for two other profiles. If the plasma scale-length is longer (e.g., the red dot-dashed curve) than the optimum, the bunch focuses sooner (red solid line) than the vacuum focus and if the scale-length is shorter (e.g., the dark-blue curve) it focuses later into the plasma (dark-blue solid
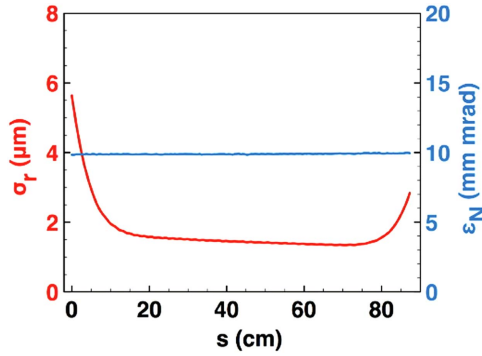
Figure 10. Beam spot size variation (red curve) and the emittance variation (blue line) throughout the plasma with matching sections. Values are full projections of the trailing bunch. The vacuum waist size occurs at $s = 0$ cm and the injected bunch has a normalized emittance of 10 μm.

line). In either case the mismatched beams execute betatron oscillations in the plasma, unlike the matched beam that propagates without oscillating. The maximum spot size of the mismatched bunches will be larger than that of the matched bunch and they will therefore emit more betatron radiation. Figure 9(b) shows one way to quantify this mismatch; e.g., the ratio of the maximum spot size to the matched spot size versus ramp scale-length (similar plots can be made for errors in the waist location or size). To the extent that a mismatch produces more betatron radiation, fine-tuning of the beam and/or positioning of the plasma ramps and profile can be accomplished by minimizing the measured betatron radiation. In principle, the subsequent down-ramp should have a profile slightly different than that at the entrance. However, the matched beam size goes like $\gamma^{-1/4}$ so even a doubling of the trailing beam's energy does not significantly affect the matching out of the plasma.

In addition to the beam loading and final energy of the two bunches shown in figure 7, we show in figure 10 the variation of the beam emittance and the beam spot size as observed in the same QuickPIC simulation. As expected by using the plasma matching sections (the ramps) the normalized emittance of the beam is indeed preserved throughout the injection, acceleration and beam extraction process. Using the experimentally measured ramp profile of figure 8(b) and with $\varepsilon_N = 10\ \mu$m, the Twiss parameters of the two bunches were initialized to produce a (vacuum) $\beta^* = 3.9$ cm ($\sigma^* = 4.4\ \mu$m) and the proper σ^* as found from the procedure discussed for figure 8. The other beam parameters used in the simulation are given in the caption of figure 7. The spot-size variation seen in figure 10 shows how the trailing beam remains matched (following a $\sim \gamma^{1/4}$ trend) into and out of the plasma despite the fact that its energy continuously varies. But the most important result is that the normalized beam emittance does not increase within the ramps or throughout the acceleration process, as shown by the red curve in figure 10.

4.4. Generation of ultralow emittance beams

Although the FACET II facility will provide beams that have more than an order of magnitude smaller emittance than the FACET I facility beams, these beams will not have the super low emittance required for a future collider or light source application. We will therefore explore if plasma wakefield structures themselves are capable of producing ultralow emittance beams. Several ideas have been proposed in the literature; here we discuss several that are particularly promising for testing at FACET II.

4.4.1. Localized ionized injection. Ionization injection of electrons was first discovered in the early PWFA experiments on FFTB when He buffer gas atoms confining the Li gas vapor (in a heat pipe oven) were ionized in the density upramp region. In this transition region the He density rapidly decreases as the Li density increases [25]. Unfortunately these ramps were typically 10 cm long. Consequently the initially mismatched bunch underwent multiple betatron oscillations and produced a secondary (ionization injected) beam from He electrons that had a large energy spread. This result was confirmed in FACET I experiments that produced up to 25 GeV beams with an emittance as low as 5 μm—a factor of 10 smaller than the emittance of the drive beam but once again a fairly large ($\pm 10\%$) energy spread [36]. Computer simulations show that if the He injection region can be localized such that the drive electron bunch only undergoes one betatron oscillation while traversing the He and that the peak electric field of the bunch at the betatron focus just exceeds the He ionization threshold, the emittance and the energy spread of the ionized He electrons can be further reduced by a factor of 5. The parameters of the FACET II beam (a smaller initial emittance leading to a few micron spot size) are ideal to ionize a column of hydrogen that has within it a 1 cm long region embedded with He atoms emanating from a H/He gas jet.

4.4.2. Density down-ramp injection using beam parameters at FACET II. It is well known that a sudden density transition from a high-to-low-density region will trap plasma electrons in the wake [37]. Even if the density transition is relatively gradual, electrons can be trapped as the wavelength of the wake adiabatically increases [38]. We have examined the possibility of generating ultra-low emittance beams using a beam driver going across a density downramp via 3D PIC code simulations. We use a FACET II-like drive beam with dimensions $10 \times 10 \times 10\ \mu$m, and charge of 1 nC. The plasma density drops from $2.9 \times 10^{17}\ \mathrm{cm}^{-3}$ down to $2.2 \times 10^{17}\ \mathrm{cm}^{-3}$ over a down-ramp length of 260 μm. The results of this simulation are shown in figure 11. The emittance of the 10 GeV injected bunch is 120×120 nm and the injected bunch has a correlated energy spread with a mean energy gain of 150 MeV. The beam charge, peak current, and brightness are 230 pC, 27 kA, and $3.8 \times 10^{18}\ \mathrm{A\ rad}^{-2}\ \mathrm{m}^{-2}$, respectively.

The density downramp injection method could potentially be used to investigate the injection of so called 'flat beams' in the wake. Many designs of e^-e^+ linear colliders utilize flat beams having extremely disparate emittances in the two transverse directions. The idea here is to use an elliptical
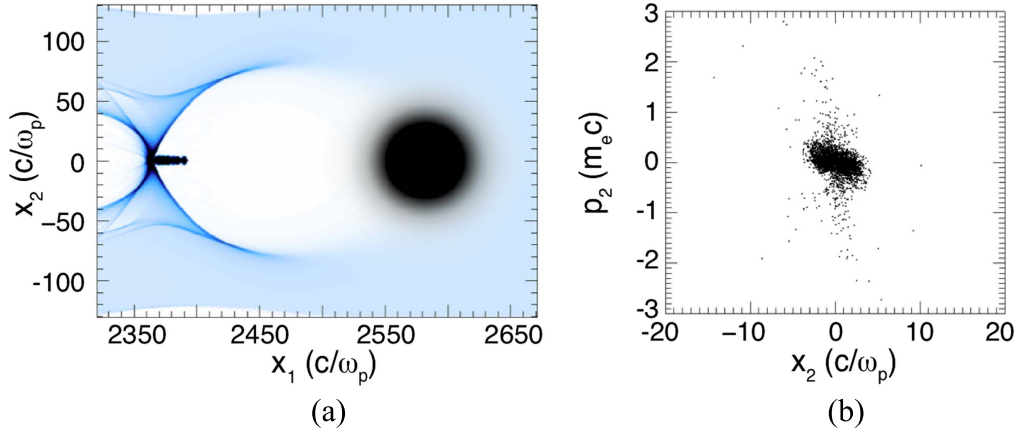
Figure 11. (a) Simulation results of density down ramp injection with a 1 nC, $10 \times 10 \times 10 \, \mu m$, 10 GeV beam driver. The plasma density is varied from $2.9 \times 10^{17} \, cm^{-3}$ down to $2.2 \times 10^{17} \, cm^{-3}$ and the down ramp length is 260 μm. (a) Electron density distribution (in blue) shows the bubble-like wake and the drive bunch and the narrow, trailing injected bunch (in black) are traveling from left to right. (b) x_2–p_2 phase space of the injected beam core. The unit simulation length in this figure is $c/\omega_p \sim 1$ micron and the charge is $\sim$230 pC (displayed at a time of 2770 ω_p^{-1}). The emittance of the total beam is 120×120 nm. The peak current and brightness are 27 kA and $3.8 \times 10^{18} \, A \, rad^{-2} \, m^{-2}$ respectively. (Courtesy Fei Li and Wei Lu Tsinghua University & UCLA).
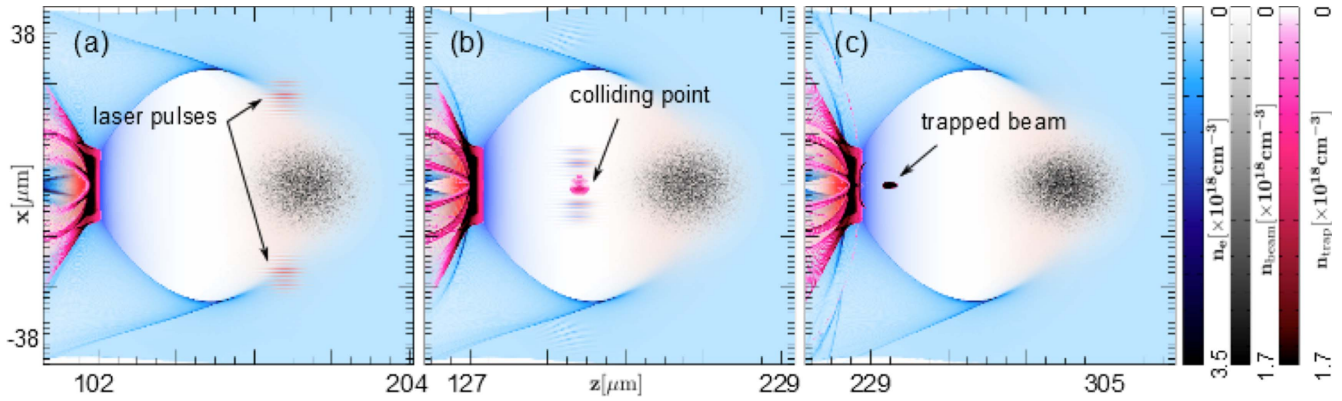

Figure 12. Snapshots from PIC code simulations illustrating the transverse colliding pulse injection of helium electrons into the ion cavity. Snapshots (a)–(c) show the charge density distribution of driver beam, wake electrons and helium electrons at three different times (a) $\sim$80 fs before laser pulses collision; (b) around laser pulses' collision time; and (c) $\sim$200 fs after collision when the injected electrons become trapped in the wake. (Courtesy Fei Li and Wei Lu Tsinghua University & UCLA).

drive bunch to generate a similarly elliptical fully blown-out wake across the density ramp. The goal is to generate much lower emittance asymmetric bunches when injection occurs in the downramp. If such beams can be generated then the next challenge would be to see if such a bunch can be accelerated in the PWFA while maintaining its differing emittance in the two orthogonal directions.

4.4.3. Ultralow emittance bunch generation by transversely colliding laser injection scheme. Generation of low emittance electron bunches has been tested at FACET I using the so-called Trojan Horse scheme [39] wherein a longitudinally co-propagating laser pulse ionizes and injects electrons inside an electron beam driven wake. On FACET II we propose to test a variation of this scheme that has the potential to generate even lower emittance (higher brightness) beams. We call this the transversely colliding laser injection method [40]. Here ultra-bright electron bunches are produced using ionization injection triggered by two transversely colliding laser pulses inside a beam-driven wake. The relatively low intensity lasers

are polarized along the wake axis and overlap with the wake for a very short time. The result is that the residual momentum of the ionized electrons in the transverse plane of the wake is much reduced and the injection is localized along the propagation axis of the wake to the spot size of the overlapping beams. This minimizes both the initial 'thermal' emittance and the emittance growth due to longitudinal phase mixing. This concept is successfully tested through 3D particle-in-cell (PIC) simulations. In figure 12 we show the injection process of helium electrons by two colliding laser pulses in a wake formed in a partially ionized He plasma by an electron beam. We show that an ultra-short ($\sim$8 fs) high-current (0.4 kA) electron bunch with normalized emittances of 8 and 6 nm in the two planes with a brightness greater than $1.7 \times 10^{19} \, A \, rad^{-2} \, m^{-2}$ can be obtained for realistic parameters.

The transverse colliding pulse injection is inherently more complex than the density down ramp injection. Here we now have to deal with femtosecond synchronization of two laser ultra-short laser pulses that must overlap with one

another within a micron inside the wake. In either scheme electrons could potentially be accelerated to multi-GeV level within roughly 10 cm. How will one measure the emittance of such a beam? Perhaps the most conclusive demonstration that the beam has a brightness exceeding $10^{19}\,A\,rad^{-2}\,m^{-2}$ will be to send this beam through a section of an undulator and measure gain of the self amplified spontaneous emission. This is currently being studied through integrated PIC and FEL simulations [41].

4.5. In situ generation and acceleration of positrons during FACET II-Phase 1

Initially, FACET II will not have a positron capability (future incorporation of e^+ was discussed briefly in section 3). Therefore any near-term experiments on positron acceleration must involve a single experiment that generates, captures, and accelerates a positron beam that is generated by the existing electron beam(s). A two-electron bunch configuration that we use for electron acceleration experiments has been shown to be ideal for generating positron beams with an identical temporal structure when focused on a high Z foil [42]. If the foil is placed at the entrance of a plasma wake then the strong focusing force of the plasma wake can capture some of these positrons and accelerate them at a high gradient. Such an experiment can be tried out on FACET II using a molybdenum foil inserted in a rubidium heat pipe oven. The extremely low ionization potential of the Rb ensures that even though the electrons scatter in the molybdenum foil, their transverse electric field will be intense enough to ionize the Rb atoms and form the wake. The importance of this experiment is that it will allow the exploration of an alternate approach to studying positron plasma interaction that covers the entire range of linear to highly nonlinear PWFA regimes while positron-bunch capabilities become available on FACET II.

5. Conclusion

In this paper we have described the PWFA research and development plan on the FACET II facility that is under construction at SLAC. The first experiments, guided by simulations, will begin in 2019 and will continue until 2025. Pump depletion of the drive beam, energy doubling of the 10 GeV trailing beam, high drive bunch to the trailing bunch energy transfer efficiency, and understanding of the factors that may cause emittance growth are the main goals of the first phase of the PWFA program. This will be complemented by experiments that aim to generate ultralow emittance beams that are needed for the demonstration of an early practical application of a PWFA and exploration of an alternate scheme for positron generation, coupling, and acceleration in a plasma.

ORCID iDs

C Joshi ⬤ https://orcid.org/0000-0002-1696-9751
W An ⬤ https://orcid.org/0000-0003-3829-3526

References

[1] Joshi C and Katsouleas T 1985 Laser acceleration of particles *AIP Conf. Proc.* **130**
[2] Adli E, Delahaye J-P, Gessner S J, Hogan M J, Raubenheimer T, An W, Joshi C and Mori W 2013 A beam driven plasma-wakefield linear collider: from Higgs factory to multi-TeV *Proc. Community Summer Study 2013: Snowmass on the Mississippi (CSS2013)* (arXiv:1308. 1145v2 [physics.acc-ph])
[3] Leemans W P and Esaray E 2009 Laser-driven plasma-wave electron accelerators *Phys. Today* **62** 44
[4] Tajima T and Dawson J M 1979 Laser electron accelerator *Phys. Rev. Lett.* **43** 267
[5] Chen P, Dawson J M, Huff R W and Katsouleas T 1985 Acceleration of electrons by the interaction of a bunched electron beam with a plasma *Phys. Rev. Lett.* **54** 693
[6] Joshi C 2006 Plasma accelerators *Sci. Am.* **294** 41
[7] Esarey E, Shroader C B and Leemans W P 2009 Physics of laser-driven plasma-based accelerators *Rev. Mod. Phys.* **81** 1229
[8] Litos M *et al* 2014 High-efficiency acceleration of an electron beam in a plasma wakefield accelerator *Nature* **515** 92
[9] Leemans W P *et al* 2014 Multi-GeV electron beams from capillary-discharge-guided subpetawatt laser pulses in the self-trapping regime *Phys. Rev. Lett.* **113** 245002
[10] Building for Discovery, Strategic Plan for US Particle Physics in the Global Context The Particle Physics Project Prioritization Panel (P5). Subpanel of the High Energy Physics Advisory Panel (HEPAP) 2014 http:// usparticlephysics.org/p5/

[11] SLAC Site Office 2015 *Preliminary Conceptual Design Report for the FACET-II Project* SLAC-R-1067 SLAC National Accelerator Laboratory (http://inspirehep.net/record/1466563)

[12] Joshi C *et al* 2002 High energy density plasma science with an ultrarelativistic electron beam *Phys. Plasmas* **9** 1845

[13] Green S Z *et al* 2014 Laser ionized preformed plasma at FACET *Plasma Phys. Control. Fusion* **56** 084011

[14] O'Connell C *et al* 2006 Plasma production via field ionization *Phys. Rev. Spec. Top.—Accel. Beams* **9** 101301

[15] Rosenzweig J B, Breizman B, Katsouleas T and Su J J 1991 Acceleration and focusing of electrons in two-dimensional nonlinear plasma wake fields *Phys. Rev.* A **44** R6189

[16] Lu W, Huang C, Zhou M, Mori W B and Katsouleas T 2006 Nonlinear theory for relativistic plasma wakefields in the blowout regime *Phys. Rev. Lett.* **96** 165002

[17] Clayton C *et al* 2016 Self-mapping the longitudinal field structure of a nonlinear plasma accelerator activity *Nat. Commun.* **7** 12483

[18] Blumenfeld I *et al* 2007 Energy doubling of 42 GeV electrons in a metre-scale plasma wakefield accelerator *Nature* **445** 741

[19] Blue B E *et al* 2003 Plasma-wakefield acceleration of an intense positron beam *Phys. Rev. Lett.* **90** 214801

[20] Clayton C E *et al* 2002 Transverse envelope dynamics of a 28.5 GeV electron beam in a long plasma *Phys. Rev. Lett.* **88** 154801

[21] Muggli P *et al* 2004 Meter-scale plasma-wakefield accelerator driven by a matched electron beam *Phys. Rev. Lett.* **93** 014802

[22] Wang S *et al* 2002 X-ray emission from betatron motion in a plasma wiggler *Phys. Rev. Lett.* **88** 135004

[23] Johnson D K *et al* 2006 Positron production by x rays emitted by betatron motion in a plasma wiggler *Phys. Rev. Lett.* **97** 175003

[24] Hogan M J *et al* 2003 Ultrarelativistic-positron-beam transport through meter-scale plasmas *Phys. Rev. Lett.* **90** 205002

[25] Oz E *et al* 2007 Ionization-induced electron trapping in ultra-relativistic plasma wakes *Phys. Rev. Lett.* **98** 084801

[26] Emma P and LCLS Commissioning Team 2009 First lasing of the LCLS x-ray FEL at 1.5 Å *Proc. Particle Accelerator Conf. (Vancouver BC, Canada)* p 3115 (http://inspirehep.net/record/1378993)

[27] Litos M *et al* 2016 9 GeV energy gain in a beam-driven plasma wakefield accelerator *Plasma Phys. Control. Fusion* **58** 034017

[28] Corde S *et al* 2015 Multi-gigaelectronvolt acceleration of positrons in a self-loaded plasma wakefield *Nature* **524** 442

[29] Doche A *et al* 2017 Acceleration of a trailing positron bunch in a plasma wakefield accelerator *Sci. Rep.* **7** 14180

[30] Gessner S *et al* 2016 Demonstration of a positron beam-driven hollow channel plasma wakefield accelerator *Nat. Commun.* **7** 11785

[31] Gessner S *et al* Acceleration of a trailing positron bunch in a hollow channel plasma wakefield accelerator (in preparation)

[32] Lindstrøm C A *et al* 2017 Measurement of transverse wakefields in hollow plasma channels *Phys. Rev. Lett.* submitted

[33] Grand Challenges for Engineering 2008 National Academy of Engineering http://engineeringchallenges.org/8965.aspx

[34] Tzoufras M, Lu W, Tsung F S, Huang C, Mori W B, Katsouleas T, Vieira J, Fonseca R A and Silva L O 2008 Beam loading in the nonlinear regime of plasma-based acceleration *Phys. Rev. Lett.* **101** 145002

[35] Xu X L *et al* 2016 Physics of phase space matching for staging plasma and traditional accelerator components using longitudinally tailored plasma profiles *Phys. Rev. Lett.* **116** 124801

[36] Najafabadi N *et al* 2016 Evidence for high-energy and low-emittance electron beams using ionization injection of charge in a plasma wakefield accelerator *Plasma Phys. Control. Fusion* **58** 034009

[37] Suk H, Barov N, Rosenzweig J B and Esarey E 2001 Plasma electron trapping and acceleration in a plasma wake field using a density transition *Phys. Rev. Lett.* **86** 1011

[38] Xu X L, Li F, An W, Yu P, Lu W, Joshi C and Mori W B 2017 High quality electron bunch generation using a longitudinal density-tailored plasma-based accelerator in the three-dimensional blowout regime *Phys. Rev. Accel. Beams* **20** 111303

[39] Hidding B, Pretzler G, Rosenzweig J B, Königstein T, Schiller D and Bruhwiler D L 2012 Ultracold electron bunch generation via plasma photocathode emission and acceleration in a beam- driven plasma blowout *Phys. Rev. Lett.* **108** 035001

[40] Li F *et al* 2013 Generating high-brightness electron beams via ionization injection by transverse colliding lasers in a plasma-wakefield accelerator *Phys. Rev. Lett.* **111** 015003

[41] Xinlu X 2017 private communication

[42] Wang X, Ischebeck R, Muggli P, Katsouleas T, Joshi C, Mori W B and Hogan M J 2008 Positron injection and acceleration on the wake driven by an electron beam in a foil-and-gas plasma *Phy. Rev. Lett.* **101** 124801